

Joint Design of Transmit Waveforms and Receive Filters for MIMO Radar via Manifold Optimization

Huanyu Zhang

ShanghaiTech University

School of Information Science and Technology

Shanghai, China

zhanghy4@shanghaitech.edu.cn

Ziping Zhao

ShanghaiTech University

School of Information Science and Technology

Shanghai, China

zhaoziping@shanghaitech.edu.cn

Abstract—The problem of joint design of transmit waveforms and receive filters is desirable in many application scenarios of multiple-input multiple-output radar systems. In this paper, the joint design problem is investigated under the signal-to-interference-plus-noise ratio (SINR) performance metric, in which case the problem is formulated to maximize the SINR at the receiver side subject to some practical transmit waveform constraints. A numerical algorithm is proposed for problem resolution based on the manifold optimization method, which has been shown to be powerful and flexible to address nonconvex constrained optimization problems in many engineering applications. The proposed algorithm is able to efficiently solve the SINR maximization problem with different waveform constraints under a unified framework. Numerical experiments demonstrate the proposed algorithm outperforms the existing benchmarks in terms of computation efficiency and achieves comparable SINR performance.

Index Terms—MIMO system, SINR maximization, waveform constraints, manifold optimization, Riemannian gradient descent.

I. INTRODUCTION

Multiple-input multiple-output (MIMO) radar systems have attracted a lot of attentions due to its flexibility in transmitting different waveforms through multiple transmit antennas [1]. For different application scenarios, the waveforms in a MIMO radar system can be properly designed to achieve a desired target measured by a specific performance criterion, which may not be possible in the classical phased-array radar systems [2]. Hence, the intriguing property of waveform diversity has provided the MIMO radars numerous appealing features like higher resolution property and better parameter identifiability property.

The problem of joint design of transmit waveforms and receive filters is desirable in many application scenarios of the MIMO radar systems. In this paper, we study the joint design problem to maximize the signal-to-interference-plus-noise ratio (SINR) performance metric at the system receiver side subject to some practical transmit waveform constraints [3], [4]. The problem is intrinsically nonconvex due to the highly nonconvex fractional objective and the nonconvex waveform constraints. Since no analytical solution to the SINR maximization problem can be attained, many iterative algorithms have been applied to solve it in the literature. One of the classical methods is the sequential optimization

algorithm combined with the semidefinite relaxation (SDR) with randomization for rank-1 solution reconstruction [5]. Solving an SDR in each iteration has been argued to incur high computational complexity [6], which is not applaudable and amenable to large-scale problems and real-time signal processing applications. In order to reduce the complexity, a widely used method is to resort to the majorization-minimization (MM) method [7]. The MM method converts the original nonconvex problem to a series of relatively simpler problems to be solved in each iteration by choosing a proper upper-bound function. The MM-based algorithm has been shown to be efficient for the SINR maximization problem [8]. Besides, due to its flexibility in choosing the upper-bound function, the MM-based algorithm is able to handle various practical waveform constraints which are not feasible by SDR method.

Recently, the manifold optimization has shown its advantages in dealing these nonconvex optimization problems for applications in many engineering fields [9]. In manifold optimization, amounts of constrained optimization problems in the Euclidean space can be regarded as unconstrained optimization problems on the manifolds [10]. Therefore, unconstrained optimization methods (such as the gradient descent) can be implemented on the manifold. Similar to other fields, manifold optimization methods have been exploited for problem solving in MIMO radar systems. In [11], a manifold optimization method called Riemannian gradient descent (RGD) has been applied for transmit beampattern synthesis under the unimodular constraint which is modeled as the complex circle manifold (CMM). However, besides unimodular constraint there are several other waveform constraints which have practical applicability with the consideration of hardware configuration. Besides that, there are few literature studying the joint design of transmit waveforms and receive filters for SINR maximization problem [5], [8], [12]. In this paper, the SINR maximization problem will be studied based on manifold optimization under multiple waveform constraints, where the projection operators and the retraction operators of each manifolds are leveraged to handle the waveform constraints. Numerical results depict that the proposed structure-aware algorithm outperforms the state-of-the-art methods in terms of computation efficiency and is able to achieve comparable SINR's. Recently, there is an independent research work on manifold optimization for the SINR maximization problem [13], which is different from this paper in some aspects. First, this paper considers several waveform constraints in the problem formulation. However,

This work was supported in part by the National Nature Science Foundation of China (NSFC) under Grant 62001295 and in part by the Shanghai Sailing Program under Grant 20YF1430800.

[13] only considers the constant modulus constraint. Second, two papers are different in problem formulations. This paper considers SINR formulation for colocated radars; however, [13] considers airborne colocated radars for the MIMO-STAP setting [14]. Third, although both papers are based on the high-level conceptual idea of manifold, the algorithms proposed are quite distinct. This paper chooses first to reduce the receiver variable and then to optimize the waveform vector as a single-block optimization problem. However, [13] directly optimizes the receiver and waveform vector on the product manifold. Forth, two papers are different in the numerical comparisons, where this paper gives a detailed numerical comparisons with several existing algorithms, namely, SDR and two MM-based algorithms, but [13] only compares with SDR.

II. JOINT TX-RX DESIGN FOR SINR MAXIMIZATION

A MIMO radar system with N_t transmit antennas and N_r receive antennas is considered. Each transmit antenna can emit individual waveform and the n -th sample emitted from the N_t transmitters is $\mathbf{s}(n) = [s_1(n), \dots, s_{N_t}(n)]^T \in \mathbb{C}^{N_t}$ with $n = 1, \dots, N$, where N denotes the total number of transmitted samples. The range-angle position of the target to be tracked is configured as (r_0, θ_0) and usually we set $r_0 = 0$. Additionally, K signal-dependent interferers located at (r_k, θ_k) are also taken into account with the range position $r_k \in \{0, \dots, N\}$ and the spatial angle $\theta_k \in \{0, \dots, L\} \times \frac{2\pi}{L+1}$ for $\theta_k \neq \theta_0$ with $k = 1, \dots, K$ and L denoting the number of discrete azimuth sectors. Therefore, the signals at the receive antennas can be represented by

$$\mathbf{x}(n) = \alpha \mathbf{a}_r(\theta_0) \mathbf{a}_t(\theta_0)^T \mathbf{s}(n) + \mathbf{d}(n) + \mathbf{v}(n), \quad (1)$$

for $n = 1, \dots, N$. In Eq. (1), α is the complex amplitude of the target with $\mathbb{E} [|\alpha|^2] = \sigma_\alpha^2$, and $\mathbf{a}_r(\theta) \in \mathbb{C}^{N_r}$ and $\mathbf{a}_t(\theta) \in \mathbb{C}^{N_t}$ are the propagation vector and the steering vector, respectively with $\mathbf{a}_t(\theta) = \frac{1}{\sqrt{N_t}} [e^{-j\pi \sin \theta}, \dots, e^{-j\pi(N_t-1) \sin \theta}]^T$ and $\mathbf{a}_r(\theta) = \frac{1}{\sqrt{N_r}} [e^{-j\pi \sin \theta}, \dots, e^{-j\pi(N_r-1) \sin \theta}]^T$ with the transmit and receive antennas are both assumed to be uniform linear arrays with half-wavelength separation. The term $\mathbf{d}(n)$ denotes the K signal-dependent uncorrelated point-like interferers as $\mathbf{d}(n) = \sum_{k=1}^K \alpha_k \mathbf{a}_r(\theta_k) \mathbf{a}_t(\theta_k)^T \mathbf{s}(n - r_k)$, where α_k denotes a complex amplitude with $\mathbb{E} [|\alpha_k|^2] = \sigma_k^2$. The term $\mathbf{v}(n) \in \mathbb{C}^{N_t}$ is a noise term with covariance $\sigma_v^2 \mathbf{I}_{N_t}$.

Let $\mathbf{x} = [\mathbf{x}(1)^T, \dots, \mathbf{x}(N)^T]^T$, $\mathbf{s} = [\mathbf{s}(1)^T, \dots, \mathbf{s}(N)^T]^T$, and $\mathbf{v} = [\mathbf{v}(1)^T, \dots, \mathbf{v}(N)^T]^T$. We obtain the following compact signal model as

$$\mathbf{x} = \alpha \mathbf{A}(r_0, \theta_0) \mathbf{s} + \sum_{k=1}^K \alpha_k \mathbf{A}(r_k, \theta_k) \mathbf{s} + \mathbf{v}, \quad (2)$$

where $\mathbf{A}(r_k, \theta_k) = [\mathbf{I}_N \otimes (\mathbf{a}_r(\theta_k) \mathbf{a}_t(\theta_k)^T)] \mathbf{J}_{r_k}$ with $k = 0, \dots, K$ is a Hermitian matrix with respect to position r_k and angle θ_k with a shift matrix $\mathbf{J}_{r_k} \in \mathbb{R}^{N_t N \times N_t N}$ given by

$$[\mathbf{J}_{r_k}]_{m,n} = \begin{cases} 1, & m - n = N_t r_k \\ 0, & m - n \neq N_t r_k \end{cases} = [\mathbf{J}_{-r_k}^T]_{m,n}.$$

For notational simplicity, we denote $\mathbf{A}(r_k, \theta_k) = \mathbf{A}_k$ hereafter.

Let $\mathbf{w} \in \mathbb{C}^{N_r N}$ be the response receive filters, the SINR [15] at the receiver side can be calculated as

$$\text{SINR} = \frac{\sigma_0^2 |\mathbf{w}^H \mathbf{A}_0 \mathbf{s}|^2}{\mathbf{w}^H (\sum_{k=1}^K \sigma_k^2 \mathbf{A}_k \mathbf{s} \mathbf{s}^H \mathbf{A}_k^H) \mathbf{w} + \sigma_v^2 \mathbf{w}^H \mathbf{w}}. \quad (3)$$

Finally, the joint design of transmit waveforms and receive filters for SINR maximization (TxRx-SINR) problem is given as

$$\begin{aligned} & \underset{\mathbf{s}, \mathbf{w}}{\text{maximize}} && \frac{|\mathbf{w}^H \mathbf{A}_0 \mathbf{s}|^2}{\mathbf{w}^H \sum_{k=1}^K \vartheta_k \mathbf{A}_k \mathbf{s} \mathbf{s}^H \mathbf{A}_k^H \mathbf{w} + \mathbf{w}^H \mathbf{w}} \quad (\text{TxRx-SINR}) \\ & \text{subject to} && \mathbf{s} \in \mathcal{M}, \end{aligned}$$

where $\vartheta_k = \sigma_k^2 / \sigma_v^2 > 0$, and \mathcal{M} denotes different considered waveform constraints to be detailed in the next section.

III. ALGORITHMIC FRAMEWORK

A. Optimization over a manifold

Consider a constrained optimization problem as follows:

$$\underset{x}{\text{minimize}} \quad f(x) \quad \text{subject to} \quad x \in \mathcal{R},$$

where \mathcal{R} is a constraint set treated as a Riemannian manifold embedded in an Euclidean space $\mathcal{E} \supseteq \mathcal{R}$ equipping the Riemannian metric [10]. Optimizing $f(x)$ can be regarded as an unconstrained optimization problem in the manifold \mathcal{M} rather than a constrained one with explicit constraint \mathcal{R} in the Euclidean space. Hence, numerous unconstrained optimization algorithms like the gradient descent [16] can be utilized to handle these manifold optimization problems.

In this paper, the gradient descent algorithm, a classical unconstrained optimization method, will be implemented for optimization over the Riemannian manifold, which hence is named as Riemannian gradient descent (RGD) [10]. The idea of RGD can be summarized as follows. Given an initialization $x^{(0)}$, a sequence $\{x^{(i)}\}$ is generated by RGD through iteratively taking two steps until convergence. The first step is “descent with projection” where the gradient of any smooth extension of the objective function, i.e., $\tilde{f}(x)$ with $x \in \mathcal{E}$ is computed as $\nabla \tilde{f}(x^{(i)})$, i.e., the standard gradient in the Euclidean space, then the Riemannian (manifold) gradient is obtained by projecting $\nabla \tilde{f}(x^{(i)})$ onto the tangent space $T_{x^{(i)}} \mathcal{M}$ by an orthogonal projection at $x^{(i)}$ denoted by $\text{Proj}_{x^{(i)}}(\cdot)$, and finally $\bar{x}^{(i)}$ is obtained by a descent step on $T_{x^{(i)}} \mathcal{M}$ with the direction $\text{Proj}_{x^{(i)}}(\nabla \tilde{f}(x^{(i)}))$ and a prespecified stepsize $\alpha^{(i)}$. Due to the updated $\bar{x}^{(i+1)}$ is on $T_{x^{(i)}} \mathcal{M}$ rather than the manifold \mathcal{M} , a “retraction” at $\bar{x}^{(i)}$ denoted by the operator $\text{Retr}(\cdot)$ is applied in the second step to map it back to \mathcal{M} . To summarize, the update step of RGD at the i -th iteration is

$$\begin{cases} \bar{x}^{(i+1)} = x^{(i)} - \gamma^{(i)} \text{Proj}_{x^{(i)}}(\nabla \tilde{f}(x^{(i)})) \\ \hspace{15em} \text{[descent with projection]} \\ x^{(i+1)} = \text{Retr}(\bar{x}^{(i+1)}) \\ \hspace{15em} \text{[retraction]}, \end{cases}$$

where the stepsize $\gamma^{(i)}$ can be chosen to be constant or according to a specific stepsize rule like the Armijo backtracking line search [17] for convergence guarantee, and the projection operator $\text{Proj}_{x^{(i)}}(\cdot)$ and the retraction operator $\text{Retr}(\cdot)$ may vary from manifolds.

$$\begin{aligned}
\nabla \bar{g}(\mathbf{s}) &= -2 \left(\mathbf{A}_0^H \left(\sum_{k=1}^K \vartheta_k \mathbf{A}_k \mathbf{s} \mathbf{s}^H \mathbf{A}_k^H + \mathbf{I} \right)^{-1} \mathbf{A}_0 \mathbf{s} \right) + 2\gamma \mathbf{s} - \left(\mathbf{s}^H \frac{\partial}{\partial \mathbf{s}} \left(\mathbf{A}_0^H \left(\sum_{k=1}^K \vartheta_k \mathbf{A}_k \mathbf{s} \mathbf{s}^H \mathbf{A}_k^H + \mathbf{I} \right)^{-1} \mathbf{A}_0 \right) \right) \mathbf{s} \\
&= -2 \left(\mathbf{A}_0^H \left(\sum_{k=1}^K \vartheta_k \mathbf{A}_k \mathbf{s} \mathbf{s}^H \mathbf{A}_k^H + \mathbf{I} \right)^{-1} \mathbf{A}_0 \mathbf{s} \right) + 2\gamma \mathbf{s} - \left(\mathbf{1}_{NN_t} \otimes \mathbf{s}^H \mathbf{A}_0^H \left(\sum_{k=1}^K \vartheta_k \mathbf{A}_k \mathbf{s} \mathbf{s}^H \mathbf{A}_k^H + \mathbf{I} \right)^{-1} \right) \\
&\quad \times \sum_{k=1}^K \left(\vartheta_k \mathbf{I}_{NN_t} \otimes \mathbf{A}_k \left[\frac{\partial \mathbf{s} \mathbf{s}^H}{\partial s_1} \cdots \frac{\partial \mathbf{s} \mathbf{s}^H}{\partial s_{NN_t}} \right]^T \mathbf{A}_k^H \right) \left(\sum_{k=1}^K \vartheta_k \mathbf{A}_k \mathbf{s} \mathbf{s}^H \mathbf{A}_k^H + \mathbf{I} \right)^{-1} \mathbf{A}_0 \mathbf{s}
\end{aligned} \tag{4}$$

B. The projection and retraction operators in TxRx-SINR

In this section, we consider the projection operators and the retraction operators w.r.t. different manifold constraints \mathcal{M} 's encountered in the Problem (TxRx-SINR). Three commonly used manifold constraints are considered which are highly nonconvex in the Euclidean space, namely the constant modulus (CM) constraint $\mathcal{M}_c = \{\mathbf{s} \mid |s_n| = \frac{1}{\sqrt{NN_t}}\}$ [18] (including the unimodular constraint, i.e., the CM with $|s_n| = 1$), the ϵ -uncertainty constant modulus (ϵ -CM) constraint $\mathcal{M}_e = \{\mathbf{s} \mid c_m - \epsilon_1 < |s_n| < c_m + \epsilon_2 \text{ with } 0 \leq \epsilon_1 \leq c_m \text{ and } 0 \leq \epsilon_2\}$ [19], and the constant modulus and similarity (CM&S) constraint $\mathcal{M}_s = \{\mathbf{s} \mid |s_n| = \frac{1}{\sqrt{NN_t}}, \|\mathbf{s} - \mathbf{s}_{\text{ref}}\|_\infty \leq \epsilon, \text{ with } 0 \leq \epsilon \leq \frac{2}{\sqrt{NN_t}}\}$ [20].

The projection operator. The projection operator $\text{Proj}_{\mathcal{M}}^{(i)}(\cdot)$ at the iterate $\mathbf{s}^{(i)} \in \mathcal{M}$ with \mathcal{M} taking \mathcal{M}_c 's or \mathcal{M}_s 's is the same and has a closed-form solution. This result is classical in manifold optimization and can be easily proved by first showing the complex scalar case and then extending it to the complex vector case [10]. For any $\mathbf{u} \in \mathbb{C}^{NN_t}$, the projection operator for these two constraints is given by

$$\text{Proj}_{\mathcal{M}}^{(i)}(\mathbf{u}) = \mathbf{u} - \text{Re} \left\{ \mathbf{u}^* \odot \mathbf{s}^{(i)} \right\} \odot \mathbf{s}^{(i)} \odot \frac{1}{|\mathbf{s}^{(i)}|}, \tag{5}$$

where \odot denotes the Hadamard product. The ϵ -CM constraint describes an annulus manifold, the projection operator of which is given by

$$\text{Proj}_{\mathcal{M}}^{(i)}(\mathbf{u}) = \mathbf{u}, \tag{6}$$

The retraction operator. The retraction operators $\text{Retr}(\cdot)$'s w.r.t. different \mathcal{M} 's can be solved in closed-forms. For a given $\mathbf{u} \in \mathbb{C}^{NN_t}$, a unified retraction function can be employed to handle all the manifold constraints, which is given by

$$\text{Retr}(\mathbf{u}) = \arg \min_{\mathbf{s} \in \mathcal{M}} \|\mathbf{s} - \mathbf{u}\|_2, \tag{7}$$

where specifically the solution w.r.t. \mathcal{M}_c is given by $\text{Retr}(\mathbf{u}) = \mathbf{u} \odot (\sqrt{NN_t}|\mathbf{u}|)^{-1}$ with $|\cdot|$ and $(\cdot)^{-1}$ applied element-wisely, w.r.t. \mathcal{M}_s can be found in [21], and w.r.t. \mathcal{M}_e is given in [19].

IV. SOLVING THE TxRx-SINR PROBLEM VIA RGD

Now we are ready to derive the RGD algorithm for Prob. (TxRx-SINR). Noting that this problem is invariant to a scaling in \mathbf{w} , i.e., if \mathbf{w} is optimal to Prob. (TxRx-SINR), then so is $a\mathbf{w}$ with $a \neq 0$. For a fixed \mathbf{s} , the resolution of \mathbf{w} can be transformed to be a convex problem as follows:

$$\begin{aligned}
&\underset{\mathbf{w}}{\text{minimize}} \quad \mathbf{w}^H \left[\sum_{k=1}^K \vartheta_k \mathbf{A}_k \mathbf{s} \mathbf{s}^H \mathbf{A}_k^H + \mathbf{I} \right] \mathbf{w} \quad (\text{Rx Prob.}) \\
&\text{subject to} \quad \mathbf{w}^H \mathbf{A}_0 \mathbf{s} = 1,
\end{aligned}$$

to which a closed-form solution for \mathbf{w} is obtained by [22]

$$\mathbf{w}^* = \frac{\left[\sum_{k=1}^K \vartheta_k \mathbf{A}_k \mathbf{s} \mathbf{s}^H \mathbf{A}_k^H + \mathbf{I} \right]^{-1} \mathbf{A}_0 \mathbf{s}}{\mathbf{s}^H \mathbf{A}_0^H \left[\sum_{k=1}^K \vartheta_k \mathbf{A}_k \mathbf{s} \mathbf{s}^H \mathbf{A}_k^H + \mathbf{I} \right]^{-1} \mathbf{A}_0 \mathbf{s}}. \quad (\text{Optim. Rx})$$

Substituting (Optim. Rx) into the original Prob. (TxRx-SINR), we get the subproblem for the transmit waveforms as

$$\begin{aligned}
&\underset{\mathbf{s}}{\text{minimize}} \quad -\mathbf{s}^H \mathbf{A}_0^H \left[\sum_{k=1}^K \vartheta_k \mathbf{A}_k \mathbf{s} \mathbf{s}^H \mathbf{A}_k^H + \mathbf{I} \right]^{-1} \mathbf{A}_0 \mathbf{s} \quad (\text{Tx Prob.}) \\
&\text{subject to} \quad \mathbf{s} \in \mathcal{M},
\end{aligned}$$

where the waveform constraints \mathcal{M} can take different forms as discussed in Sec. III-B.

To solve the original Prob. TxRx-SINR, it suffices to solve the Prob. (Tx Prob.) for \mathbf{s} and then obtain \mathbf{w} by (Optim. Rx). In this paper, we propose to solve (Tx Prob.) via the RGD method as introduced in Sec. III-A. For convergence concern, the objective of problem (Tx Prob.) will be augmented with a constant term $\gamma \mathbf{s}^H \mathbf{s}$ (γ is a prescribed constant, the choice of which guarantees the monotonicity of ‘‘projection’’ step in RGD) to control the monotonicity of the retraction operator $\text{Retr}(\cdot)$. Then we define the ‘‘augmented’’ objective function for problem (Tx Prob.) as

$$g(\mathbf{s}) = -\mathbf{s}^H \left(\mathbf{A}_0^H \left[\sum_{k=1}^K \vartheta_k \mathbf{A}_k \mathbf{s} \mathbf{s}^H \mathbf{A}_k^H + \mathbf{I} \right]^{-1} \mathbf{A}_0 \right) \mathbf{s} + \gamma \mathbf{s}^H \mathbf{s}.$$

The gradient of a smooth extension of the objective function denoted by $\bar{g}(\mathbf{s})$ (extending $g(\mathbf{s})$ to the Euclidean domain) is given in (4) where \otimes denotes the Kronecker product and $\frac{\partial \mathbf{s} \mathbf{s}^H}{\partial s_n}$ ($n = 1, \dots, NN_t$) is a matrix calculated by $\frac{\partial \mathbf{s} \mathbf{s}^H}{\partial s_n} = [\mathbf{s}, \mathbf{0}, \dots, \mathbf{0}] \mathbf{J}_{r_k/N_t} + \mathbf{J}_{r_k/N_t}^T [\mathbf{s}, \mathbf{0}, \dots, \mathbf{0}]^H$ with the shift matrix $\mathbf{J}_{r_k/N_t} \in \mathbb{R}^{N_t N \times N_t N}$ defined in Sec. II.

Finally, the proposed RGD algorithm for TxRx-SINR is summarized in Algorithm 1¹.

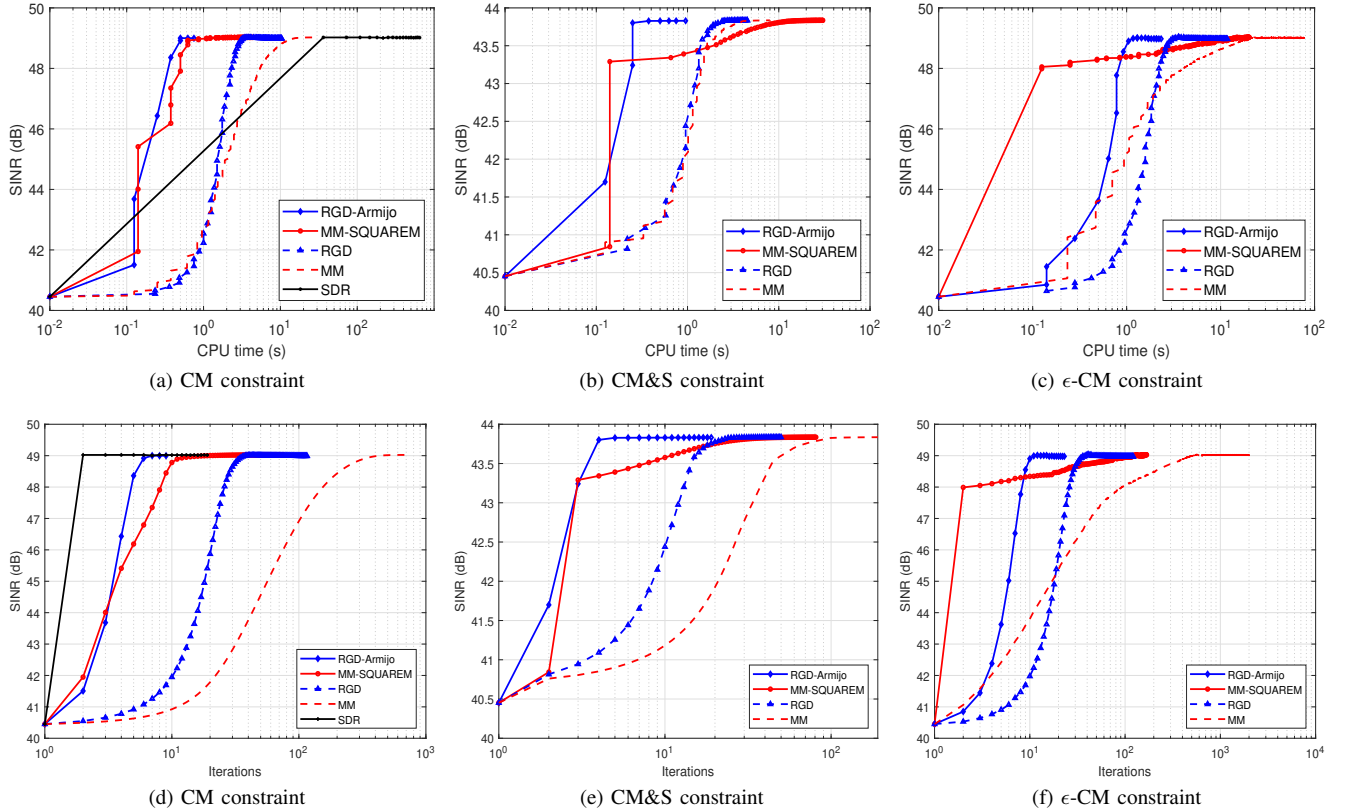


Fig. 1: Convergence rate comparisons.

Algorithm 1 Solving TxRx-SINR problem via RGD

Initialize: $i = 0$, $\mathbf{s}^{(0)}$, γ , β , τ , σ

While not converge do

1. Compute $\nabla \bar{g}(\mathbf{s}^{(i)})$ according to Eq. (4)
2. Compute $\text{Proj}_{\mathcal{S}_k}(\nabla g(\mathbf{s}^{(i)}))$ according to Eq. (5) or Eq. (6)
- 3-1. [constant stepsize] $\gamma^{(i)} = \gamma$
- 3-2. [Armijo back-tracking linesearch [17]] $\gamma^{(i)} = \tau \beta^m$ with m the smallest non-negative integer such that

$$g(\mathbf{s}^{(i)}) - g(\mathbf{s}^{(i)} - \tau \beta^m \nabla g(\mathbf{s}^{(i)})) \geq \sigma \tau \beta^m \|\text{Proj}_{\mathcal{S}^{(i)}}(\nabla g(\mathbf{s}^{(i)}))\|_2^2$$

4. $\bar{\mathbf{s}}^{(i+1)} = \mathbf{s}^{(i)} - \gamma^{(i)} \text{Proj}_{\mathcal{S}^{(i)}}(\nabla g(\mathbf{s}^{(i)}))$
5. $\mathbf{s}^{(i+1)} = \text{Retr}(\bar{\mathbf{s}}^{(i+1)})$ according to (7)
6. $i = i + 1$

end while

Compute \mathbf{w} according to (Optim. Rx)

V. NUMERICAL EXPERIMENTS

In this section, we compare the performance of our proposed RGD algorithm with the state-of-the-art methods in the literatures. The simulation is conducted on the MATLAB2019b platform under a PC machine with an Intel i7-10700 CPU and 16GB RAM. For the MIMO radar system settings, the range-angle position of the target to be tracked is configured as $(0, 15^\circ)$, the power of which is $|\alpha_0|^2 = 30\text{dB}$. Three fixed

¹A well-chosen stepsize $\gamma^{(i)}$ is to ensure the decrease of the objective function $g(\cdot)$ in the “descent with projection” step of RGD.

TABLE I: Runtime comparisons under CM constraint.

Algorithm	(N_r, N_t, N)				
	(4,4,4)	(10,10,4)	(10,10,8)	(15,15,8)	(10,10,30)
RGD-Armijo	0.0197sec.	0.3729sec.	0.7536sec.	4.3909sec.	74.3386sec.
MM-SQUAREM	0.7969sec.	1.2813sec.	2.2971sec.	29.7969sec.	518.7628sec.
RGD	0.7031sec.	3.7134sec.	10.3421sec.	173.4153sec.	1026.127sec.
MM	1.875sec.	4.0156sec.	20.3203sec.	207.6719sec.	1231.6143sec.
SDR	35.1021sec.	31.4375sec.	431.7156sec.	620.8147sec.	2029.9058sec.

interferers are located at the range-angle positions $(0, -50^\circ)$, $(1, -10^\circ)$, and $(2, 40^\circ)$, respectively. The power of each interferer is $|\alpha_j|^2 = 20\text{dB}$ for $j = 1, 2, 3$. The variance of the noise is $\sigma_v^2 = 0\text{dB}$. The orthogonal linear frequency modulation (LFM) waveforms are set as the initial and also the reference waveforms in the CM&S constraint. The space-time LFM waveform matrix is

$$\mathbf{S}^{(0)}(k, n) = \frac{e^{j2\pi k(n-1)/N} e^{j\pi(n-1)^2/N}}{\sqrt{N N_t}}, \quad (8)$$

where $k = 1, \dots, N_t$ and $n = 1, \dots, N$, based on which we obtain the initialization iteration $\mathbf{s}^{(0)} = \text{vec}(\mathbf{S}^{(0)})$.

We first compare the performance of the TxRx-SINR problem with CM constraint between the two proposed algorithms, i.e., the RGD algorithm and the RGD with Armijo rule denoted as RGD-Armijo (for parameters in the Armijo back-tracking rule, we have set $\sigma = 1$, $\beta = 0.85$, and $\tau = 0.4$) with the benchmark methods, namely SDR, MM, and MM with SQUAREM acceleration denoted as MM-SQUAREM under

three different waveform constraints. The collocated MIMO radar parameters are chosen as $N_t = 10$, $N_r = 10$, and $N = 8$. In Fig. 1a, it can be shown that all methods converge to the same SINR. As expected, SDR is the most time-consuming one. RGD-Armijo converges faster than RGD and both of them perform better than MM. MM-SQUAREM is much faster than MM due to the acceleration scheme, but is still slower than RGD-Armijo. Similar convergence results are observed for the TxRx-SINR problem with other constraints, namely the CM&S constraint (similarity parameter $\epsilon = 1/\sqrt{N_t N}$), and the ϵ -CM constraint, which are shown in Fig. 1b and Fig. 1c, respectively.

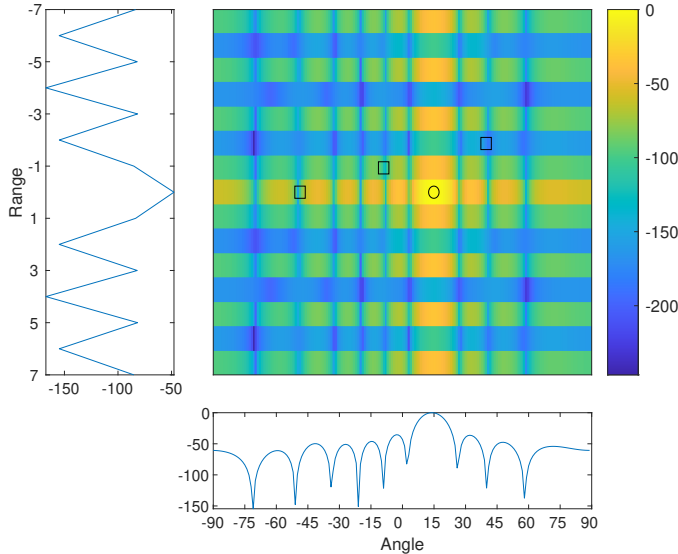


Fig. 2: Range-angle ambiguity function for CM constraint.

To further test the scalability of the proposed algorithms, cases with different (N, N_r, N_t) are evaluated with comparisons to the benchmark methods under the CM constraint. The runtimes are reported in Table I. To evaluate the performance of the MIMO ambiguity function shaping via the designed waveforms from our proposed RGD algorithm. We plot the ambiguity function (the expression of ambiguity function is chosen as in [23]) in Fig. 2, which can capture the inherent resolution properties of the MIMO radar systems [24]. In Fig. 2, it can be observed that the ambiguity function resembles a thumbtack, the maximum value of which is located at $(0, 15^\circ)$ marked by a circle. For the interferers, their locations are marked by rectangles. Values of interferers in the ambiguity function are relatively small. Fig. 2 also provides the angle slice at the range $r = 0$ and the range slice at the angle $\theta = 15^\circ$. It can be observed that there are cliffs at angle $\theta = 40^\circ, -10^\circ$, and -50° with range $r = 2$.

VI. CONCLUSIONS

In this paper, we have considered the SINR maximization problem in MIMO radar subject to multiple practical waveform constraints by jointly designing the transmit waveforms and receive filters. A manifold optimization algorithm called RGD is proposed for problem resolution. Numerical results validate the superiority of the proposed algorithms.

REFERENCES

- [1] J. Li and P. Stoica, Eds., *MIMO radar signal processing*. Hoboken, NJ: Wiley, 2009.
- [2] J. Li and P. Stoica, "MIMO radar with collocated antennas," *IEEE Signal Processing Magazine*, vol. 24, no. 5, pp. 106–114, Sep. 2007.
- [3] Z. Zhao and D. P. Palomar, "MIMO transmit beampattern matching under waveform constraints," in *2018 IEEE International Conference on Acoustics, Speech and Signal Processing (ICASSP)*. IEEE, 2018, pp. 3281–3285.
- [4] R. Zhou, Z. Zhao, and D. P. Palomar, "Unified framework for minimax MIMO transmit beampattern matching under waveform constraints," in *ICASSP 2019-2019 IEEE International Conference on Acoustics, Speech and Signal Processing (ICASSP)*. IEEE, 2019, pp. 4150–4154.
- [5] G. Cui, H. Li, and M. Rangaswamy, "MIMO radar waveform design with constant modulus and similarity constraints," *IEEE Transactions on Signal Processing*, vol. 62, no. 2, pp. 343–353, Jan. 2014.
- [6] Z. Luo, W. Ma, A. So, Y. Ye, and S. Zhang, "Semidefinite relaxation of quadratic optimization problems," *IEEE Signal Processing Magazine*, vol. 27, pp. 20–34, 2010.
- [7] D. R. Hunter and K. Lange, "A tutorial on MM algorithms," *The American Statistician*, vol. 58, no. 1, pp. 30–37, 2004.
- [8] L. Wu, P. Babu, and D. P. Palomar, "Transmit waveform/receive filter design for MIMO radar with multiple waveform constraints," *IEEE Transactions on Signal Processing*, vol. 66, no. 6, pp. 1526–1540, Mar. 2018.
- [9] J. Hu, X. Liu, Z.-W. Wen, and Y.-X. Yuan, "A brief introduction to manifold optimization," *Journal of the Operations Research Society of China*, vol. 8, no. 2, pp. 199–248, Jun. 2020.
- [10] P.-A. Absil, R. Mahony, and R. Sepulchre, *Optimization algorithms on matrix manifolds*. Princeton: Princeton University Press, Dec. 2008.
- [11] K. Alhujaili, V. Monga, and M. Rangaswamy, "Transmit MIMO radar beampattern design via optimization on the complex circle manifold," *IEEE Transactions on Signal Processing*, vol. 67, no. 13, pp. 3561–3575, Jul. 2019.
- [12] Z. Zhao, "Joint transmit waveforms and receive filters design for large-scale MIMO beampattern synthesis," in *2020 IEEE 11th Sensor Array and Multichannel Signal Processing Workshop (SAM)*. IEEE, 2020, pp. 1–5.
- [13] J. Li, G. Liao, Y. Huang, Z. Zhang, and A. Nehorai, "Riemannian geometric optimization methods for joint design of transmit sequence and receive filter on MIMO radar," *IEEE Transactions on Signal Processing*, vol. 68, pp. 5602–5616, 2020.
- [14] B. Tang and J. Tang, "Joint design of transmit waveforms and receive filters for MIMO radar space-time adaptive processing," *IEEE Transactions on Signal Processing*, vol. 64, no. 18, pp. 4707–4722, Sep. 2016.
- [15] A. Aubry, A. DeMaio, A. Farina, and M. Wicks, "Knowledge-aided (potentially cognitive) transmit signal and receive filter design in signal-dependent clutter," *IEEE Transactions on Aerospace and Electronic Systems*, vol. 49, no. 1, pp. 93–117, Jan. 2013.
- [16] C. Lemaréchal, "Cauchy and the gradient method," *Documenta Mathematica Extra Volume ISMP*, vol. 251, p. 254, 2012.
- [17] L. Armijo, "Minimization of functions having Lipschitz continuous first partial derivatives," *Pacific J. Math.*, vol. 16, no. 1, pp. 1–3, 1966.
- [18] H. He, J. Li, and P. Stoica, *Waveform design for active sensing systems: a computational approach*. Cambridge University Press, 2012.
- [19] L. Zhao, J. Song, P. Babu, and D. P. Palomar, "A unified framework for low autocorrelation sequence design via majorization minimization," *IEEE Transactions on Signal Processing*, vol. 65, no. 2, pp. 438–453, Jan. 2017.
- [20] A. De Maio, S. De Nicola, Y. Huang, Z. Q. Luo, and S. Zhang, "Design of phase codes for radar performance optimization with a similarity constraint," *IEEE Transactions on Signal Processing*, vol. 57, no. 2, pp. 610–621, 2009.
- [21] G. Cui, X. Yu, V. Carotenuto, and L. Kong, "Space-time transmit code and receive filter design for collocated MIMO radar," *IEEE Transactions on Signal Processing*, vol. 65, no. 5, pp. 1116–1129, Mar. 2017.
- [22] S. Boyd, S. P. Boyd, and L. Vandenberghe, *Convex optimization*. Cambridge University Press, 2004.
- [23] O. Rabaste, L. Savy, M. Cattenoz, and J.-P. Guyvarch, "Signal waveforms and range/angle coupling in coherent collocated MIMO radar," in *2013 International Conference on Radar*. Adelaide, Australia: IEEE, Sep. 2013, pp. 157–162.
- [24] G. San Antonio, D. R. Fuhrmann, and F. C. Robey, "MIMO radar ambiguity functions," *IEEE Journal of Selected Topics in Signal Processing*, vol. 1, no. 1, pp. 167–177, Jun. 2007.